Electronic Supplementary Material (ESI) for Sustainable Energy & Fuels.
This journal is © The Royal Society of Chemistry 2019

Electronic Supplementary Information (ESI) for

Rationally Assembled rGO/Sn/$Na_2Zr(PO_4)_2$ Nanocomposites as High Performance Anode Materials for Lithium and Sodium Ion Batteries

Mei Ma,[a,b] Wenzhou Shen,[b] Jiali Zhang[b] and Shouwu Guo*[b]

[a]School of Materials Science and Engineering, Shanghai Jiao Tong University, Shanghai 200240, P.R. China

[b]Department of Electronic Engineering, School of Electronic Information and Electrical Engineering, Shanghai Jiao Tong University, Shanghai 200240, P.R. China

Correspondence should be addressed to: swguo@sjtu.edu.cn

Table S1 The ICP data of Sn contents in $Sn/Na_2Zr(PO_4)_2$ composites.

Composites	$SnCl_2 \cdot 2H_2O$/mmol	$NaBH_4$/mmol	(ICP) Sn/%
$Sn/Na_2Zr(PO_4)_2$-a	1	5	21.35
$Sn/Na_2Zr(PO_4)_2$-b	0.5	2.5	10.45
$Sn/Na_2Zr(PO_4)_2$-c	1.5	7.5	29.39

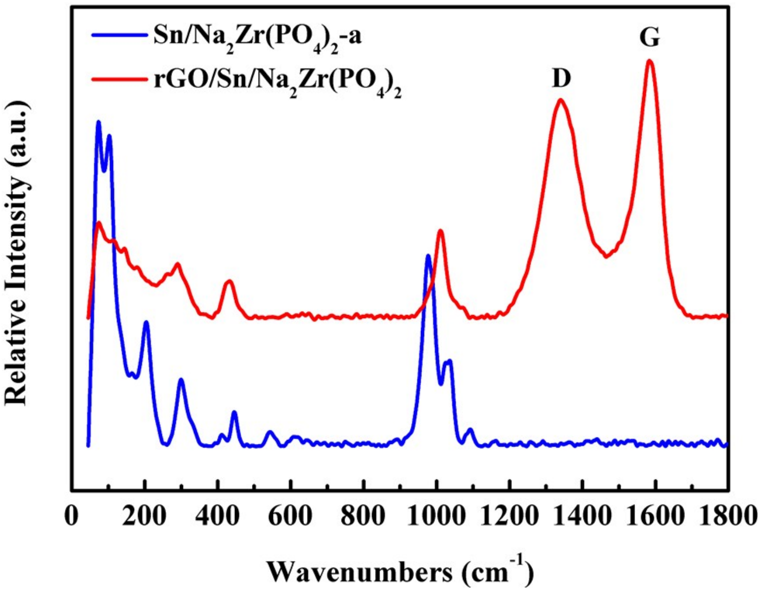

Fig. S1 Raman spectra of Sn/$Na_2Zr(PO_4)_2$-a, and rGO/Sn/$Na_2Zr(PO_4)_2$ composites. The mass fraction of rGO in the rGO/Sn/$Na_2Zr(PO_4)_2$ is 4.5%.

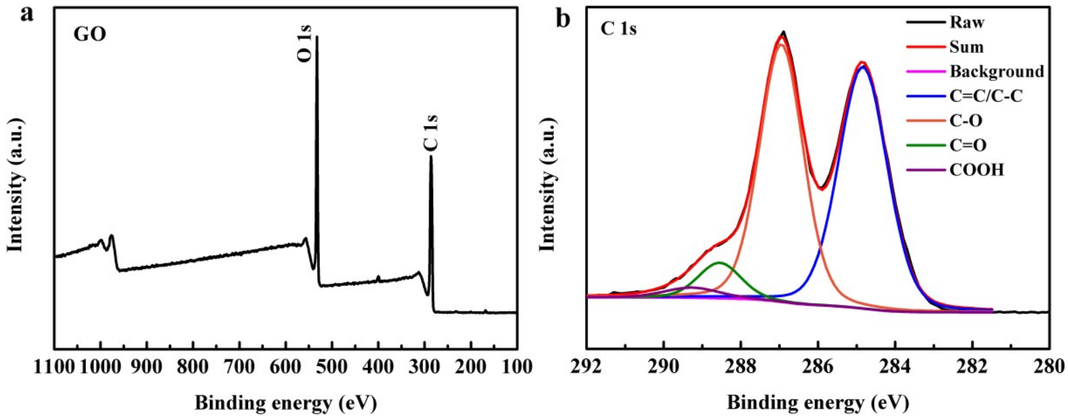

Fig. S2 XPS spectra of GO: (a) survey, (b) C 1s spectrum.

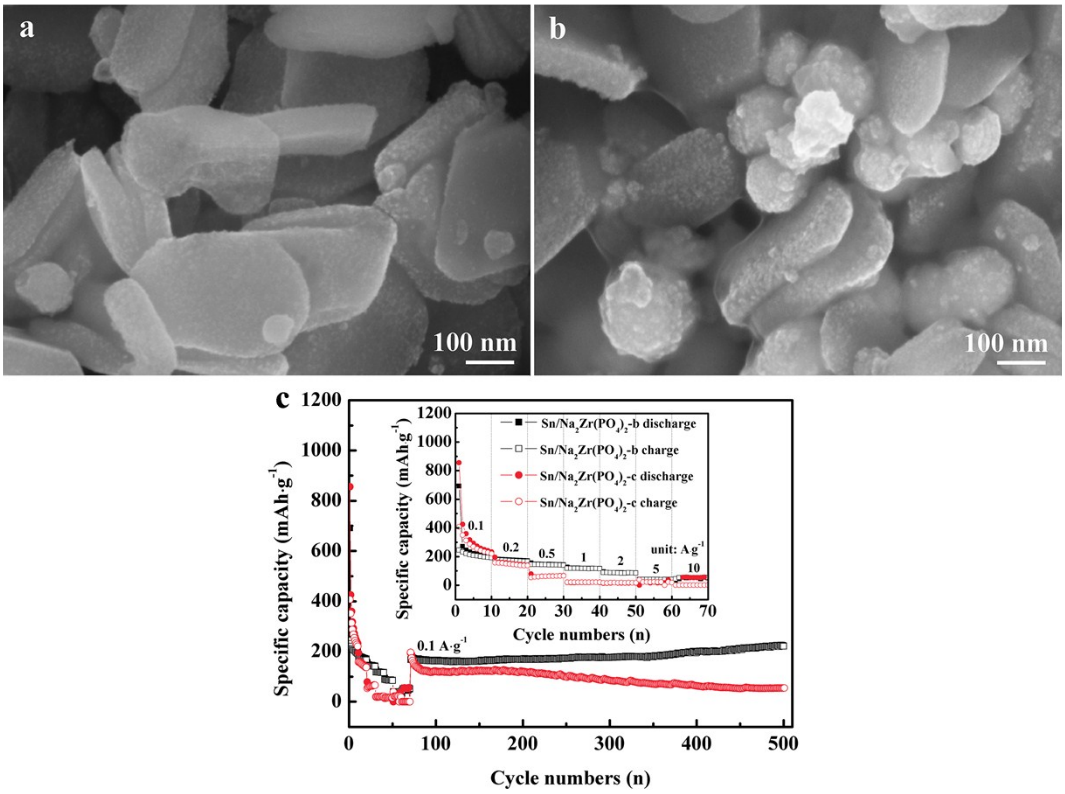

Fig. S3 SEM images of $Sn/Na_2Zr(PO_4)_2$ composites (a) $Sn/Na_2Zr(PO_4)_2$-b, and (b) $Sn/Na_2Zr(PO_4)_2$-c; (c) Galvanostatic charge/discharge curves of $Sn/Na_2Zr(PO_4)_2$-b and $Sn/Na_2Zr(PO_4)_2$-c as anodes for LIBs, measured at current densities from 0.1 A g^{-1} to 10 A g^{-1}.

Table S2 The electric resistivity of $Sn/Na_2Zr(PO_4)_2$-a, and $rGO/Sn/Na_2Zr(PO_4)_2$ composites.

Samples (bare and dry powder)	Electric Resistivity/Ω mm
$Sn/Na_2Zr(PO_4)_2$-a	1.41×10^7
$rGO/Sn/Na_2Zr(PO_4)_2$	840

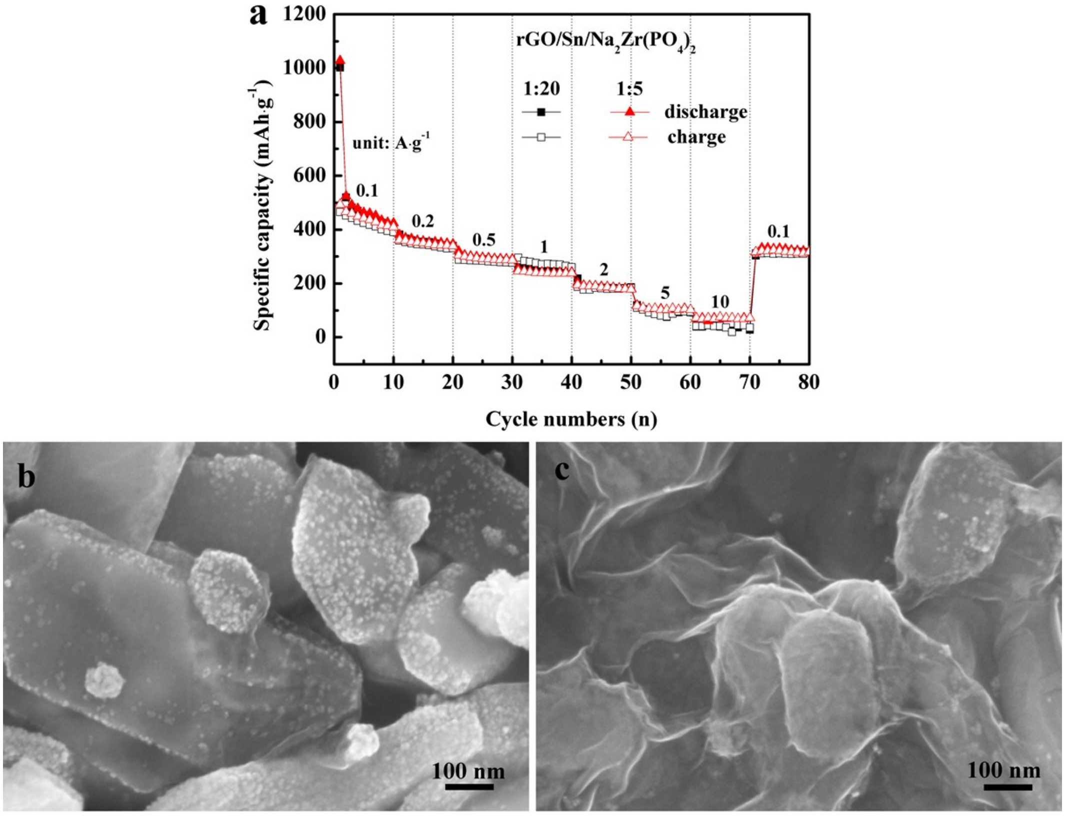

Fig. S4 (a) Galvanostatic charge/discharge curves of rGO/Sn/$Na_2Zr(PO_4)_2$ composites with different GO to Sn/[$Na_2Zr(PO_4)_2 \cdot H_2O$] ratios in weight, measured at current densities from 0.1 A g^{-1} to 10 A g^{-1}; SEM images of (b) rGO/Sn/$Na_2Zr(PO_4)_2$ (1:20), and (c) rGO/Sn/$Na_2Zr(PO_4)_2$ (1:5) composite.

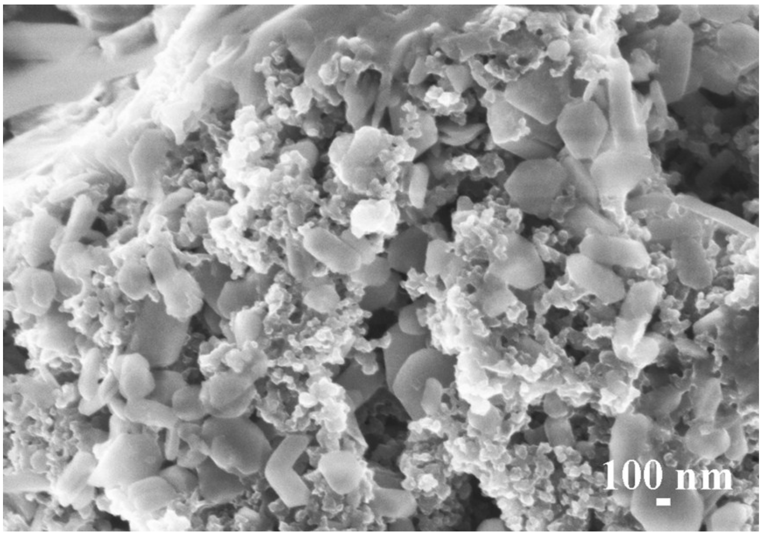

Fig. S5 SEM image of rGO/Sn/$Na_2Zr(PO_4)_2$ anode after 200 cycles at 0.1 A g^{-1}. (Note: After 200 charge/discharge cycles, coin half-cell with rGO/Sn/$Na_2Zr(PO_4)_2$ as anode was opened in an argon-filled glove box, and dimethyl carbonate (DMC) was used to wash away the residual $LiPF_6$ on the electrode surface. Afterwards, SEM was employed to analyze the morphology of the electrode material.)

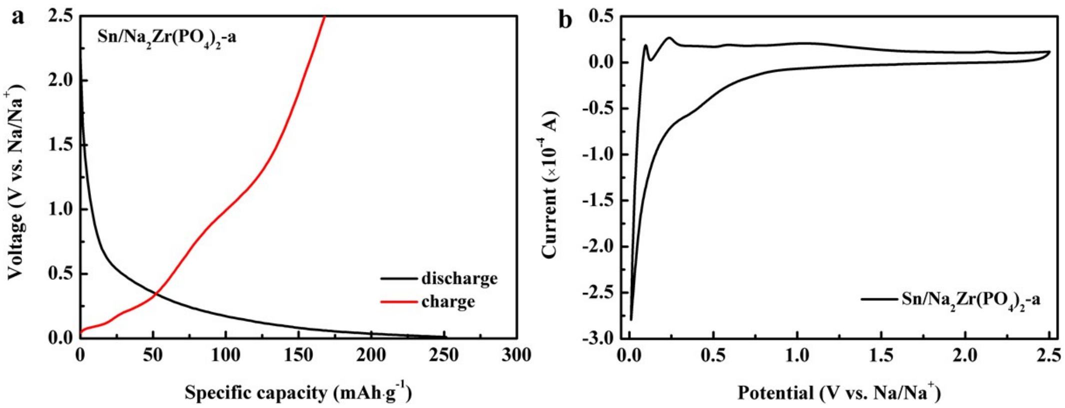

Fig. S6 (a) Charge/discharge voltage profiles of $Sn/Na_2Zr(PO_4)_2$-a at the second charge/discharge cycle measured at a current density of 0.1 A g^{-1}, and (b) the corresponding CV measured at a scanning rate of 0.5 mV s^{-1}.

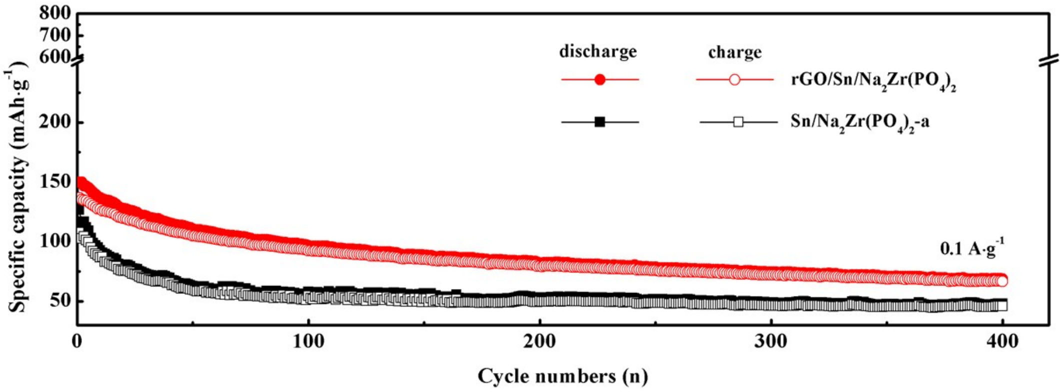

Fig. S7 Cycling performances of $Sn/Na_2Zr(PO_4)_2$-a and $rGO/Sn/Na_2Zr(PO_4)_2$ anodes, measured at a current density of 0.1 A g^{-1}.

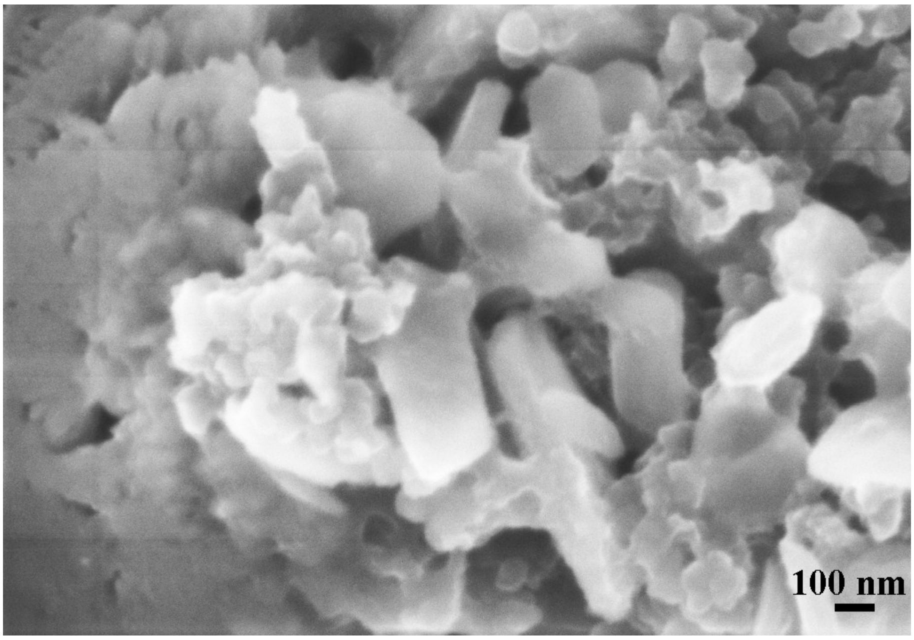

Fig. S8 SEM image of rGO/Sn/$Na_2Zr(PO_4)_2$ anode for SIB after 400 charge/discharge cycles at 0.1 A g^{-1}. (Note: After 400 charge/discharge cycles, coin half-cell with rGO/Sn/$Na_2Zr(PO_4)_2$ as anode for SIB was opened in an argon-filled glove box, and dimethyl carbonate (DMC) was used to wash away the residual $NaClO_4$ on the electrode surface. Afterwards, SEM was employed to analyze the morphology of the electrode material.)